IEEE Access
Multidisciplinary | Rapid Review | Open Access Journal

Received February 28, 2020, accepted March 9, 2020, date of publication March 12, 2020, date of current version March 24, 2020.

Digital Object Identifier 10.1109/ACCESS.2020.2980254

Hybrid Methods Based on Empirical Mode Decomposition for Non-Invasive Fetal Heart Rate Monitoring

KATERINA BARNOVA, RADEK MARTINEK, RENE JAROS, AND RADANA KAHANKOVA

Department of Cybernetics and Biomedical Engineering, Faculty of Electrical Engineering and Computer Science, VSB-Technical University of Ostrava, 70800 Ostrava, Czech Republic

Corresponding author: Rene Jaros (rene.jaros@vsb.cz)

This work was supported in part by the Ministry of Education of the Czech Republic under Project SP2020/156, and in part by the European Regional Development Fund in the Research Centre of Advanced Mechatronic Systems Project within the Operational Programme Research, Development, and Education under Grant CZ.02.1.01/0.0/0.0/16 019/0000867.

ABSTRACT This study focuses on fetal electrocardiogram (fECG) processing using hybrid methods that combine two or more individual methods. Combinations of independent component analysis (ICA), wavelet transform (WT), recursive least squares (RLS), and empirical mode decomposition (EMD) were used to create the individual hybrid methods. Following four hybrid methods were compared and evaluated in this study: ICA-EMD, ICA-EMD-WT, EMD-WT, and ICA-RLS-EMD. The methods were tested on two databases, the ADFECGDB database and the PhysioNet Challenge 2013 database. Extraction evaluation is based on fetal heart rate (fHR) determination. Statistical evaluation is based on determination of correct detection (ACC), sensitivity (Se), positive predictive value (PPV), and harmonic mean between Se and PPV (F1). In this study, the best results were achieved by means of the ICA-RLS-EMD hybrid method, which achieved accuracy (ACC) $>$ 80% at 9 out of 12 recordings when tested on the ADFECGDB database, reaching an average value of ACC $>$ 84%, Se $>$ 87%, PPV $>$ 92%, and F1 $>$ 90%. When tested on the Physionet Challenge 2013 database, ACC $>$ 80% was achieved at 12 out of 25 recordings with an average value of ACC $>$ 64%, Se $>$ 69%, PPV $>$ 79%, and F1 $>$ 72%.

INDEX TERMS Non-invasive fetal electrocardiography, fetal heart rate, hybrid methods, empirical mode decomposition (EMD), independent component analysis (ICA), wavelet transform (WT), recursive least squares (RLS).

I. INTRODUCTION

Fetal monitoring has its origins in the intermittent fetal heart sounds (fHS) auscultation, which was first documented by Kergaradec in 1822. The progress in science and technology has enabled fHS sensing in a more efficient way, allowing a better understanding of the physiology of fetal cardiac activity during uterine contractions, as well as clarifying the manifestation of fetal hypoxia (oxygen deficiency) and its influence on the fHR [1]. On the basis of these findings, the first fetal monitors based on fHS sensing using phonocardiography were introduced in the second half of the 20th century [2]. The first commercially available device (Hewlett-Packard 8020A) entered obstetric theatres in 1968, which can be considered the official beginning of electronic fetal monitoring.

Intrapartal fetal monitoring is now an integral part of modern obstetrics used to prevent fetal hypoxia. Cardiotocography (CTG), which is based on the measurement of fetal cardiac activity based on Doppler ultrasonography, is the most prevalent technique used in clinical practice. Unfortunately, this method is sensitive to fetal and maternal movement, sensor placement, or maternal body mass index (BMI) value. The actual evaluation of CTG recordings is then burdened with a large inter- and extra-observer disagreement, which is demonstrably one of the reasons for the high number of unnecessarily performed caesarean sections. Numerous studies have been trying to draw attention to these negatives for many years [3]–[6]. The efforts of the scientific community are focused on improving alternative methods

The associate editor coordinating the review of this manuscript and approving it for publication was Filbert Juwono.

for fetal monitoring, such as fetal electrocardiography, fetal phonocardiography or fetal magnetocardiography.

Fetal electrocardiography (fECG) is one of the most promising fetal monitoring techniques during pregnancy and labor. This method is based on measuring electrical potentials produced by fetal heart. This electrical energy can be sensed directly from the fetal body surface (invasively) using the so-called fetal scalp electrode, or from the surface of the mother's abdominal wall using transabdominal electrodes (non-invasively). Invasive fECG sensing offers a signal with a higher signal to noise ratio (SNR) and the ability to simultaneously sense uterine contractions using an intrauterine catheter. However, its use is limited by the necessity of the rupture of the membranes and the outflow of the amniotic fluid, which occurs only during labor. In addition, this method of monitoring is associated with a higher risk of developing infection and reduced patient comfort and mobility. In contrast, non-invasive fECG (NI-fECG) monitoring can be used throughout pregnancy and offers the possibility of safe and comfortable monitoring. The disadvantage of NI-fECG monitoring is the fact that the magnitude of the useful signal is relatively low compared to the unwanted signals contained in the abdominal recording. Thus, the greatest challenge is to suppress these interfering components, especially the maternal ECG (mECG), which overlaps with the fetal component in both time and frequency domains.

A number of extraction methods were introduced in the past. For example, blind source separation methods, such as the independent component analysis (ICA) [7] or the principal component analysis [8], are worth mentioning. Another very common approach to suppressing the maternal component comprises adaptive methods [9] which take advantage of the fact that the source of interference (mECG) is known and measurable. Recent studies have shown that the use of the individual methods is not as promising as the so-called *hybrid* systems that combine two or more of these methods [10]–[15]. Most of the techniques do not outperform the hybrid algorithms or are only effective for limited number of recordings. It is desirable to implement an algorithm that would overcome these shortcomings and be efficient for a wide range of input signals. This article presents different variations of hybrid methods combining empirical mode decomposition (EMD) with, for example, ICA, the adaptive recursive least square (RLS) algorithm, or wavelet transform (WT). The objective of this study is to create a hybrid extraction system composed of selected methods that best combines the advantages of individual algorithms while eliminating their disadvantages and limitations. Such an extraction system has the potential to achieve greater accuracy in fECG extraction, thereby improving fHR monitoring.

II. MATERIAL AND METHODS

The methods to be combined and implemented have been selected based on the literature review and the study of the issue [16]. The first method is the independent component analysis (ICA), which is able to separate mixed signals and achieves relatively good results [17]. Furthermore, it is wavelet transform (WT), which decomposes the signal by appropriately changing the width of the mother wavelet over time, and, by means of the wavelet shape, an optimum ratio of resolution in time and frequency will be achieved [18]. The RLS method is based on the calculation and minimization of the error function [19] and the EMD, which can decompose time series into intrinsic mode functions [20]. These individual methods, the databases on which the hybrid methods were tested and the evaluation parameters used in this paper will be described in more detail in the following chapters.

A. EMPIRICAL MODE DECOMPOSITION

Empirical mode decomposition is suitable for non-linear and non-stationary signals and is, therefore, also suitable for removing artifacts from the fECG signal. The aim of the method is to decompose the signal into oscillatory functions. High-frequency components are called intrinsic mode functions (IMFs) and low-frequency components are called residues [20]. The algorithm sorts functions by frequency, from highest to lowest. Two conditions must be met for the method to function properly. The number of local extremes must be the same as the number of zero crossings or must differ at most by one. The second condition is that at any point the mean value of the envelopes defined by the local maxima and the local minima must be zero [21]. The process of signal decomposition into IMFs is called sifting process and can be described by the following steps [22], [23].

First, it is necessary to identify all local maxima and minima of the input signal $s(t)$. The next step is to create appropriate envelopes, the upper envelope $e_{\max}(t)$ as a cubic spline, by linking all the maxima. Similarly, it is necessary to generate the lower envelope $e_{\min}(t)$ as a spline curve by linking all local minima [21]. The mean of envelopes is then determined according to equation (1):

$$m_{01}(t) = \frac{(e_{\min}(t) + e_{\max}(t))}{2}. \tag{1}$$

This mean value is subtracted from the input signal $s(t)$. The first proto-IMF $p_{01}(t)$ [22], [23] is obtained according to equation (2):

$$p_{01}(t) = s(t) - m_{01}(t). \tag{2}$$

Unfortunately, it does not often occur that the $p_{01}(t)$ component qualifies for IMF and it is, therefore, marked as proto-IMF at this moment. The above-stated procedure must, therefore, be repeated [22], [23]; it is generally represented by equation (3):

$$p_{\mathrm{ik}}(t) = p_{\mathrm{i(k-1)}}(t) - m_{\mathrm{ik}}(t), \tag{3}$$

where k indicates the iteration index and i the index of the extracted IMF. The procedure can theoretically be repeated until the signal size $p_{\mathrm{ik}}(t)$ is constant [23]. For this reason, it is necessary to define the stopping criterion. The process stopping criterion is defined as an estimate of the standard deviation σ [23].

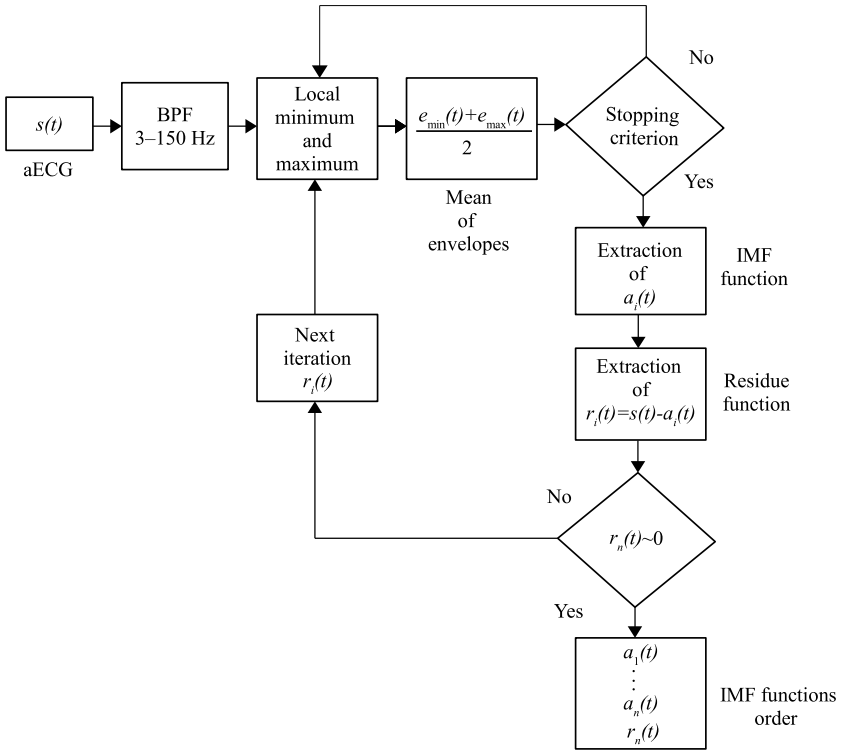

FIGURE 1. Description of the EMD principle; the formulation is a more suitable form of the algorithm than the analytical formulation. The method first locates the signal maxima and minima, determines the mean value of the envelopes, and extracts the IMF as many times as possible, until the stopping criterion is reached. This way, all IMFs are extracted; the last function is called residue. The algorithm finally sorts the individual IMFs, from the highest frequency to the lowest.

The first IMF $a_1(t)$ is obtained when σ is less than the threshold value [22]. To get more modal functions, it is necessary to repeat the whole procedure, but the residue $r_i(t)$ is used instead of the input signal $s(t)$. This is conducted by subtracting the first IMF $a_1(t)$ from the input signal $s(t)$ [22], [23]. The subtraction is defined by equation (4), where i denotes the index of the extracted IMF.

$$r_i(t) = s(t) - a_i(t). \tag{4}$$

The entire decomposition process ends when the IMF cannot be extracted from the residue $r_i(t)$. This is a state where the residue is a constant, a monotonic function, or a function with only one extreme [21]. The original signal can be reconstructed by summing all the components extracted [20], according to equation (5):

$$s(t) = \sum_{i=1}^{n} a_i(t) + r_n(t), \tag{5}$$

where $a_i(t)$ is the i-th IMF and $r_n(t)$ is the last residue, usually considered the last IMF [22], [23]. The EMD algorithm process is illustrated by the diagram shown in Fig. 1.

B. INDEPENDENT COMPONENT ANALYSIS

Independent component analysis is based on high order statistics and uses the assumption that the source signal consists of several unknown independent signals originating from different sources. The method can decompose the input signals into mutually independent non-Gaussian components. The components are sorted randomly and may be amplitude-altered [24]. There are multiple ICA-based algorithms and among them FastICA algorithm is the most commonly used. This algorithm is more efficient than the original ICA algorithm [25]. As with most ICA algorithms, FastICA aims to orthogonally rotate the predetermined data through a fixed point iteration scheme that maximizes the degree of component non-Gaussianity [17], [26]. Mathematically, the ICA method can be described according to equation (6).

$$\mathbf{x} = \mathbf{A}\mathbf{s}, \tag{6}$$

where $\mathbf{x} = [x_1, x_2, \ldots, x_n]^T$ is the multivariate signal observed, n is the number of signals observed, the unknown source signal is denoted as $\mathbf{s} = [s_1, s_2, \ldots, s_m]^T$, m is the number of source signals, and is a mixing matrix, whose lines contain transposed vectors $\mathbf{x}^T$ [24]. There are two main approaches to ICA method preprocessing, centering and whitening. The goal of the ICA algorithm is to obtain an estimate of the independent components $\mathbf{y}$ [17] using a linear, inverse, unmixing matrix $\mathbf{W}$, as described in

equation (7).

$$\mathbf{y} = \mathbf{W}\mathbf{x}. \tag{7}$$

C. WAVELET TRANSFORM

Wavelet transform is similar to the Fourier transform (FT). However, the FT method has many limitations when processing non-stationary signals. Therefore, it is suitable to use the WT method for the analysis of these non-stationary or multicomponent signals in the time-frequency domain [27]. The aim of the method is to decompose the signal by a suitable choice of the wavelet type in order to achieve an optimal ratio of resolution in time and frequency. Discrete wavelet transform (DWT) is defined by equation (8), where DWT uses dyadic grid, j is a scale parameter, k is a grid parameter and $\Psi(t)$ is a mother wavelet [27], [28]. The inverse DWT is defined by equation (9).

$$c(j,k) = \sum_{\mathrm{t}} f(t)\overline{\Psi_{\mathrm{j,k}}}(t) = 2^{\frac{\mathrm{j}}{2}}\Psi(2^{\mathrm{j}}t - k). \tag{8}$$

$$f(t) = \sum_{\mathrm{k}}\sum_{\mathrm{j}} c(j,k)\Psi_{\mathrm{j,k}}(t). \tag{9}$$

The selection of the wavelet type depends primarily on the signal to be processed. This selection is very important for achieving good results [18], [28], [29]. In this study, *Daubechies*, *Symlet*, and *Coiflet* wavelets were tested for fECG processing [29].

D. RECURSIVE LEAST SQUARES

Some adaptive methods, such as the least mean squares (LMS) algorithm, use a statistical approach to optimize the error function and require a higher number of measurements to calculate the statistics [9]. In contrast, RLS uses a deterministic approach to optimize the error function and calculates the characteristics using a large number of samples [9], [19], [30]–[32].

The RLS algorithm is based on recursive determination of weighting coefficients, KF theory, time averaging and also on the LMS algorithm. This algorithm is of very high performance because it uses the values of previous error estimates. Nevertheless, due to a large amount of data, the RLS algorithm in its basic form has higher computational demands and, in some cases, stability problems [9]. To reduce the computational demands, the RLS algorithm uses forgetting factor λ, whose task is to forget the previous values. The forgetting factor value ranges from 0 to 1 [19]. If $\lambda = 1$, no previous values are forgotten. Most often, the forgetting factor ranges from 0.98 to 1 [31]. The use of a variable forgetting factor is a frequent solution in the RLS algorithm. To reduce the computational complexity, the filter order N, which indicates the final number of the previous values processed, is selected. It is very important to set the forgetting factor and filter order well in order to make the RLS algorithm efficient and stable [30], [32]. The detailed description and implementation of the RLS algorithm can be found in [9], [19], [30]–[32].

E. METHODS SETTING

This chapter describes the settings of the individual methods. First of all, it was necessary to select appropriate combinations of the input signals. For the multichannel methods, it was necessary to select at least two abdominal signals, while the single-channel methods required one suitable input. We tested all possible combinations of input signals for each record and selected the most suitable one based on the ACC value. Moreover, individual methods include different steps and settings that need to be carried out and optimized and will be described in detail below.

1) *EMD* - the principle of the EMD method is based on decomposition of the signal into 19 oscillatory functions (IMFs). Subsequently, the most suitable IMFs are selected using an automated algorithm and summed to create an enhanced fECG. The algorithm compared the performance of fECG extraction using various combinations of IMFs. Performance comparison was carried out using the reference annotations and evaluated based on the ACC parameter. Figure 2 shows the block diagram of the EMD extraction system.
2) *ICA* - the ICA method is based on decomposing the input aECG signal into three components. In most cases, one component corresponds to the mECG signal (denoted as mECG*), the second to the aECG signal (denoted as aECG*) with the enhanced fECG component, and the third corresponds to the noise. The order of the individual components differs each time the ICA is applied. The components also alter in amplitude and are time shifted. Therefore, we used an automatic algorithm to shift and center the components and to assign components to the source signals. The assignment of the components to the source signals is based on the number of peaks detected. Finally, mECG* and aECG* components are time and amplitude aligned and standardized. The process of this algorithm is illustrated by Fig. 3 [15].
3) *WT* - for the WT method, it is important to select the wavelet type and the number of decomposition levels appropriately. The selection of the wavelet type depends primarily on the signal to be processed and it is an important factor affecting the quality of the fECG extraction [18], [28], [29]. In this study, we tested different settings of the WT-based systems, namely the decomposition levels 4 and 5 and different wavelets, such as *Daubechies*, *Symlet*, and *Coiflet*. These wavelet types have a shape similar to the QRS complex and their energy spectrum covers the range of low frequencies [29]. Before performing inverse DWT, we adjusted output signal by adaptive and soft thresholding.
4) *RLS* - when using the RLS algorithm, the filter order and the forgetting factor must be set. The grid search was used to optimize the RLS algorithm, where the filter order varied from 2 to 100 with step of 2. This way, 50 outputs of the RLS algorithm were generated

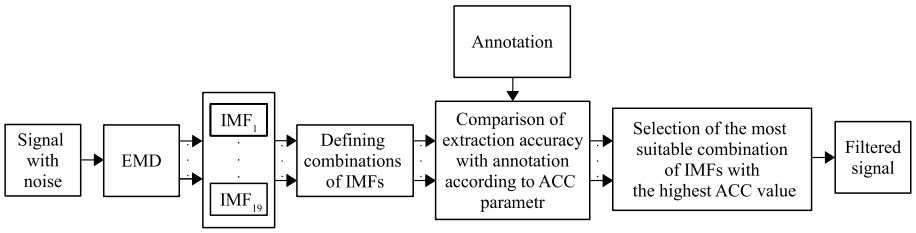

FIGURE 2. Block diagram of automatic algorithm for selecting the most suitable combination of IMFs. This algorithm compared the performance of extraction of fECG by various combinations of IMFs. Performance comparison was done according to reference annotations containing markers that accurately indicate the location of R-peaks. The evaluation parameter was ACC. The algorithm was used for hybrid methods ICA-EMD, ICA-EMD-WT and ICA-RLS-EMD.

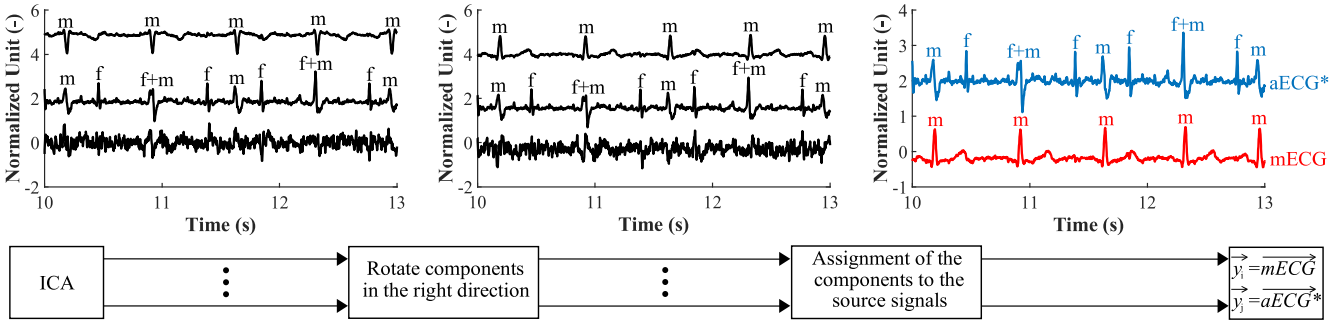

FIGURE 3. Scheme of automatic algorithm assignment of the components to the source signals, adjusting the position and polarity of ICA components.

for one electrode combination. The optimal setting of the RLS algorithm was found for each record as the global maximum of the ACC parameter [15].

F. EVALUATION PARAMETERS

The performance of individual hybrid methods in this study was evaluated by fHR statistical parameters and the accuracy of R-peak detection. First, it was necessary to determine n - the total number of fQRS complexes in the recording. This value is based on the annotation provided by experts. The FN parameter denotes false negative detection, i.e. method does not detect the fQRS complex that actually occurs in the signal. The FP parameter denotes the false positive detection, the method detects the fQRS complex that does not actually occur in the signal. Furthermore, it is possible to determine the TP parameter - True Positive, correctly detected by the fQRS complex method. The TP values correspond to the fQRS complexes detected within 50 ms interval from reference R-peak position determined by the annotation [33]. It is also possible to determine ACC - accuracy or the probability of correct detection, defined by equation (10), Se - the sensitivity of the method, defined by equation (11), PPV - positive predictive value, defined by equation (12), and F1 - total accuracy, calculated as the harmonic mean between Se and PPV, defined by equation (13) [17], [33]:

$$ACC = \frac{TP}{n} \cdot 100 = \frac{TP}{TP + FP + FN} \cdot 100\ (\%). \tag{10}$$

$$Se = \frac{TP}{TP + FN} \cdot 100\ (\%). \tag{11}$$

$$PPV = \frac{TP}{TP + FP} \cdot 100\ (\%). \tag{12}$$

$$F1 = 2 \cdot \frac{Se \cdot PPV}{Se + PPV} = \frac{2 \cdot TP}{2 \cdot TP + FP + FN} \cdot 100\ (\%). \tag{13}$$

The method is considered as accurate if the values of ACC, Se, PPV, and F1 exceed 95% [17], [34]. Depiction of fHR traces can be used to graphically assess accuracy of fECG extraction. First, it is necessary to detect the R-peaks using a detector that utilize a complex WT and to determine the RR intervals. Subsequently, a moving average is found for the values obtained by the method [17]. The more the estimated fHR trace copies the trend of the reference fHR trace, obtained using the annotations, the more successful the method was during the extraction.

Bland-Altman plots were also used to graphically compare the accuracy of the fHR detection. These plots are very often used to evaluate two methods of medical measurement [35]. The assumption is that the results of both measurements are independent. First, the differences of the two measurements are determined and the mean value of these differences is specified, then the limits of agreement (LoA) are set as the mean value of $\mu \pm 1.96\sigma$ (where σ is the standard deviation). This is an estimate of the interval in which 95% of the difference values can be expected [35]. If the values of the differences determined lie within this limit, this is an acceptable result, otherwise the value is indicated as an error [17].

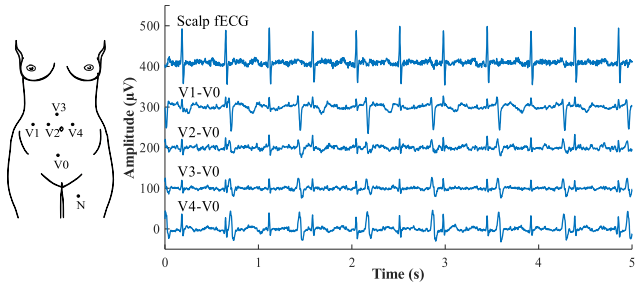

FIGURE 4. An example of the aECG signals filtered, the reference fECG signal, and the electrode layout for r01 recording. The abdominal signals are extracted using V1, V2, V3 and V4 electrodes, the reference electrode is designated V0 and N is the active grounding.

G. DATASET

For testing of hybrid methods, real recordings were obtained from twelve different women between 38 and 41 weeks of pregnancy. The recordings were extracted using four abdominal electrodes; all recordings include a reference recording from the scalp electrode. The signals were recorded using the KOMPOREL fetal electrocardiogram acquisition and analysis system (ITAM Institute, Zabrze, Poland). Five out of the twelve recordings are available in the ADFECGDB database [17], [36].

The four sensing electrodes were placed in the abdominal region, the scalp electrode was placed over the *symphysis pubica* region, and the common ground electrode was placed on the left thigh. The sampling rate was 1000 Hz for five recordings, 500 Hz for seven recordings, the bandwidth ranged from 1 to 150 Hz, and the resolution was 16 bits. Ag-AgCl electrodes were used for surface abdominal sensing and a spiral electrode for invasive scalp sensing [17]. In addition to useful signals, interference signals are also included. Most often, the source of disturbing signals is the uterine muscle activity, the maternal movements or the loss of contact of the scalp electrode with the fetal head, causing a temporary loss of signal. Therefore, only shorter, five-minute sections without signal loss were selected. An example of the aECG signals, the reference fECG signal, and the electrode layout is shown in Fig. 4 [17].

The database also includes annotations containing markers that accurately indicate the location of R-peaks. These R-peaks were determined for r01, r04, r07, r08, and r10 recordings by an on-line analysis using the KOMPOREL system and, subsequently, the placement of the markers was verified by a group of cardiologists [17].

Further testing was performed on data from set A of the Physionet Challenge 2013 database. The database contains 25 recordings, wherein each recording contains 4 aECG signals and annotations identifying the positions of R-peaks. The recording length is 1 minute, the sampling frequency is 1000 Hz and the resolution is 12 bits [37].

III. HYBRID SYSTEM DESIGN

This chapter describes the individual hybrid methods that were implemented and tested. Moreover, specific parameters that were used for a particular method are described herein. There are two different approaches used in the fECG extraction, *adaptive* and *non-adaptive*. These two approaches differ in the way of suppressing the maternal component, where the adaptive hybrid systems (ICA-RLS and ICA-RLS-EMD) use the RLS algorithm to adapt to the reference input corresponding to the maternal signal in order to subtract it from the aECG. Contrary, the *non-adaptive* systems do not contain any adaptation mechanism to extract fECG signal.

A. NON-ADAPTIVE HYBRID METHODS

Figure 5 shows a block diagram illustrating the ICA-EMD, ICA-EMD-WT, and EMD-WT hybrid systems. Figure 6 shows an example of filtration outputs using ICA-EMD, ICA-EMD-WT and EMD-WT systems. Each block can be described as follows:

- Preprocessing - first, aECG signals were filtered by a bandpass filter in the range from 3 to 150 Hz (FIR filter) in order to eliminate the baseline wander or motion artifacts.
- EMD-WT - method is a single-channel method; thus, it requires only one input signal. The EMD method decomposes aECG signal into 19 IMFs. The selection of suitable IMFs is inspired by the study of Azbari *et al.* [22], where they correlated these signals with the reference fECG signal. According to this evaluation, first 4 IMFs are the most suitable for further processing. Subsequently, a WT method is used to improve the extraction results. In terms of the system settings, the *sym10* wavelet and 4 levels of decomposition were selected as most efficient for fECG extraction.
- ICA-EMD - contrary to EMD-WT system, this hybrid extraction system includes the ICA algorithm and thus requires multiple inputs to function. The fECG extraction process using this system is composed of two steps:
  - ICA method is applied to the preprocessed signals, these input aECG signals are thus decomposed into three components. For further processing, the component corresponding to aECG signal with the enhanced fECG component (marked as aECG*) is selected.
  - EMD method is then applied to aECG* signal in order to remove the residual mECG and to enhance the fECG. The EMD method decomposes the signal into 19 IMFs. Subsequently, the most suitable IMFs are selected using the automatic algorithm described above and summed to create an enhanced fECG signal. According to the results, the most suitable combination for ICA-EMD were IMF2 and IMF4. The sum of these IMFs produces the resulting fECG.
- ICA-EMD-WT - the structure of this algorithm is similar to the previous hybrid method, however, on some IMFs, the WT method is applied to improve extraction results. Again, the most suitable functions are

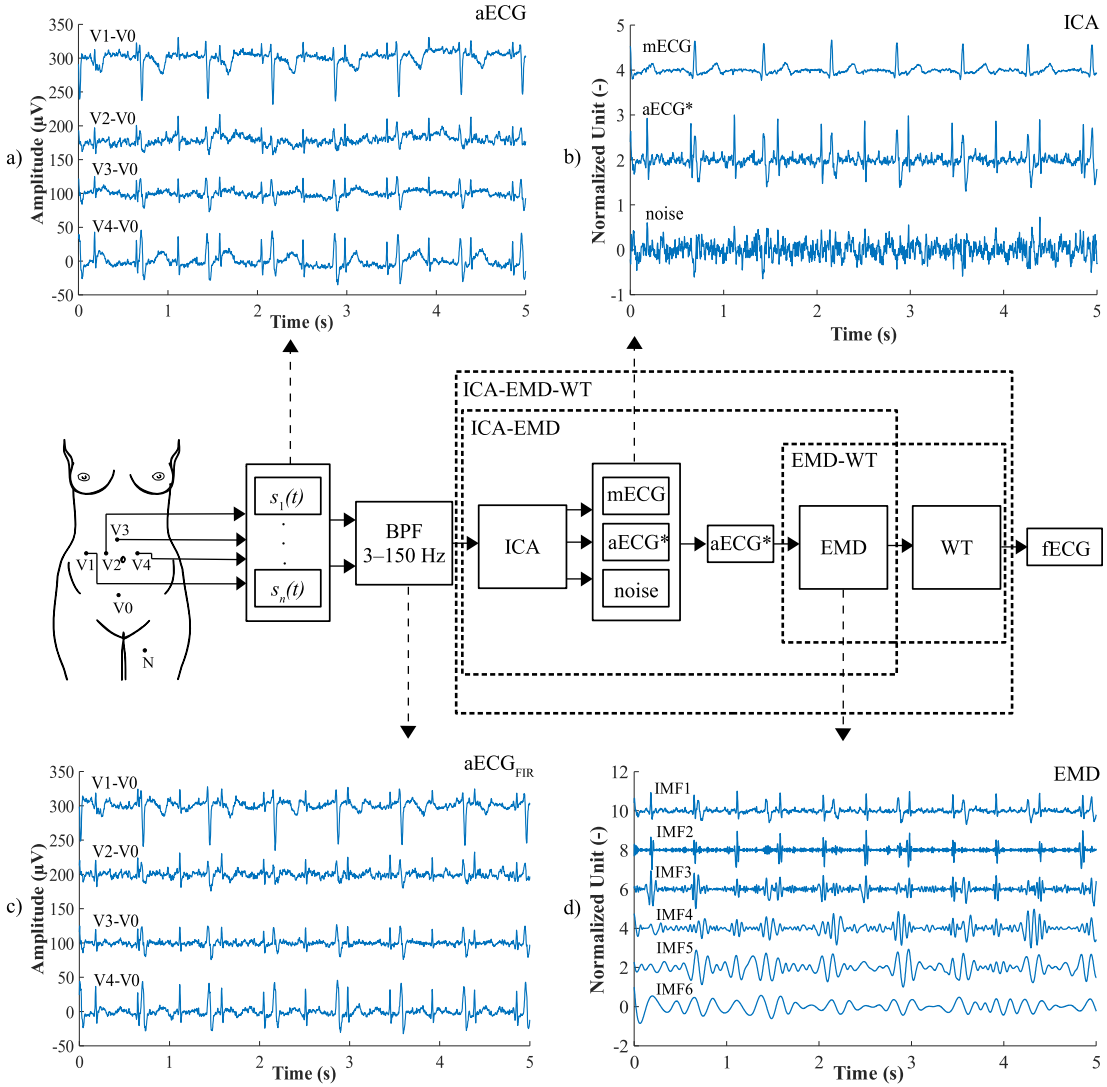

FIGURE 5. Block diagram illustrating the function of hybrid methods ICA-EMD, ICA-EMD-WT and EMD-WT with examples of the signals in individual phases: a) example of the input signal, b) example of the preproccesed input signals, c) examples of the ICA components, d) examples of the first 6 IMFs.

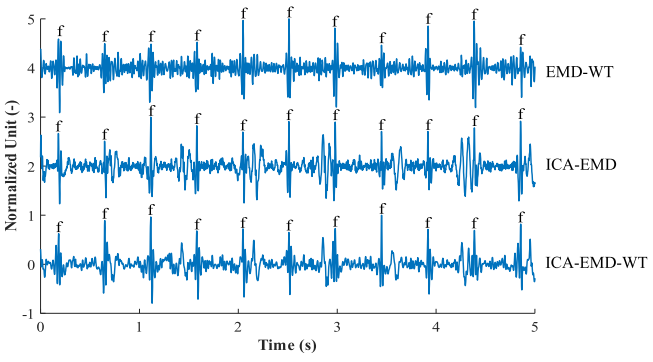

FIGURE 6. An example of fECH signals extracted using the hybrid methods ICA-EMD, ICA-EMD-WT and EMD-WT for r01 recording.

selected by automatic algorithm. The best results were achieved using following combinations: IMF1-IMF3 filtered by WT using *sym18* wavelet and 4 levels of decomposition. The original IMF4 and IMF5 (i.e. (not filtered by WT method) are then added to the filtered signals.

B. ADAPTIVE HYBRID METHODS

Finally, ICA-RLS-EMD system uses the ICA method to estimate the mECG reference signal (denoted as mECG*) and a signal denoted as aECG*. The aECG* contains the maternal component and enhanced fetal component. These signals are then used as the inputs of the adaptive block based on RLS, which is able to extract the fECG. Eventually, the EMD method is then applied to this signal in order to remove the residual noise using suitable IMFs selected using an automated algorithm. The ICA-RLS-EMD system is composed of following stages:

- Abdominal signals are extracted and filtered by a band-pass filter in the range from 3 to 150 Hz (FIR filter) in order to eliminate the variations in isolines;

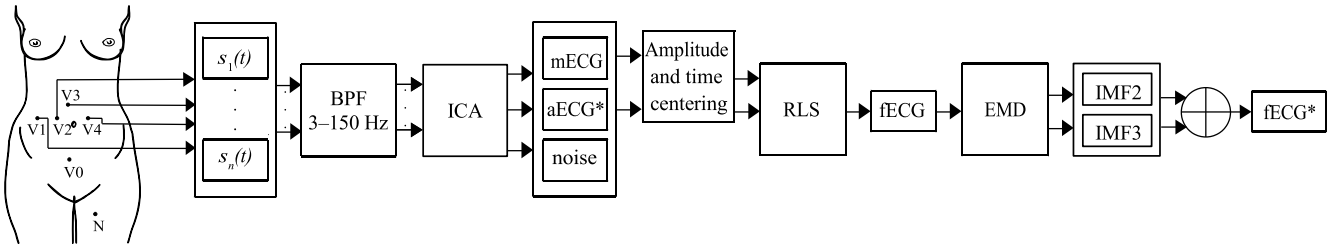

FIGURE 7. A diagram showing the principle of a combination of the ICA and EMD methods.

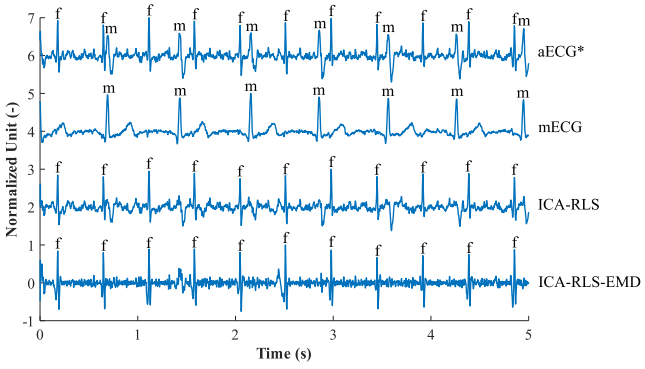

FIGURE 8. An example of the aECG* and mECG* estimates using the ICA method, an example of fECG signal extraction using the ICA-RLS and ICA-RLS-EMD algorithm for r01 recording.

- ICA method estimates the mECG* signal, the aECG* signal and the noise signal;
- mECG* signal and the aECG* signal are centered and fed to the RLS algorithm in order to extract the fECG signal.
- EMD method decomposes the signal into 19 IMFs.
- The IMF2 and IMF3 are selected and summed to contribute to the reconstruction of the improved fECG* signal.

The schematic principle of the ICA-EMD method, including the location of the sensing electrodes, is shown in Fig. 7 and Fig. 8 shows the estimated mECG and aECG* signals by ICA method, which serve as inputs to the adaptive algorithm along with the examples of output fECG signals extracted using the ICA-RLS and ICA-RLS-EMD algorithm.

IV. RESULTS

This chapter presents results of the experiments on real data obtained by the individual hybrid methods. The accuracy of R-peaks detection was evaluated using statistical parameters and graphical assessment (using Bland-Altman plots and fHR traces). The last part of this chapter compares the achieved results with other studies.

A. STATISTICAL EVALUATION

First, the EMD-WT method was evaluated. The advantage of this method is the use of only one sensing electrode, which brings more comfort to the patient than the multi-channel sensing. The TP, FP, and FN values were first determined for statistical evaluation and, based on them, the ACC, Se, PPV, and F1 parameters were calculated. The most important parameter for evaluating the extraction accuracy is the ACC parameter as the other parameters cannot be lower than ACC. The threshold for accepting the method as effective according to this parameter is usually 95%; if the method reaches 80%, these results are considered satisfactory. The results obtained using the EMD-WT method are shown in Tab. 1.

According to Tab. 1, as for the EMD-WT method, it is possible to determine that accuracy of over 95% for r01 recording and accuracy of over 80% for r08 recording was achieved by the ACC parameter. According to the Se parameter, accuracy of over 95% was achieved for r01 and r08 recordings. According to the PPV parameter, accuracy of over 95% was achieved for r01 and r08 recordings and accuracy of over 80% was received for r02 recording. According to the F1 parameter, accuracy of over 95% was achieved for r01 and r08 recordings. For other recordings, relatively low precision values were achieved and the method was not very effective for these recordings. The lowest number of FP and FN values was achieved in r01 recording. For r02 recording, the method detected a large number of FN values, causing low values of ACC, Se, and F1.

The results show that the method works correctly only with some aECG signals, usually those where the magnitude of fetal component was comparable with the maternal one (i.e. with high SNR). Thus, it was necessary to find a method that would work well for the rest of the aECG signals with lower SNR. Therefore, the ICA-EMD method, which aims to remove the residual mECG and to improve the fECG extraction by appropriately selecting IMFs, the sum of which will contribute to the generation of an improved fECG, was further tested. The method can be further improved by applying wavelet transform. This so-called ICA-EMD-WT method. The results achieved by the ICA-EMD and ICA-EMD-WT methods are in Tab. 2. The results of both methods were recorded in one table for clarity reasons.

According to Tab. 2, as for the ICA-EMD method, it is possible to determine that accuracy of over 95% for r01, r02, r05 and r08 recordings and accuracy of over 80% for r09 recording was achieved by the ACC parameter. According to the Se parameter, accuracy of over 95% was achieved for r01, r02, r05, and r08 recordings and accuracy of over

TABLE 1. Statistical evaluation of the detection of fQRS complexes obtained by the EMD-WT method that was tested on signals from the ADFECGDB database.

Recordings	Electrode	n	TP	FP	FN	ACC (%)	Se (%)	PPV (%)	F1 (%)
r01	2	644	626	8	18	96.01	97.20	98.74	97.96
r02	2	660	501	98	159	66.09	75.91	83.64	79.59
r03	4	684	91	333	593	8.95	13.30	21.46	16.42
r04	3	632	322	203	310	38.56	50.95	61.33	55.66
r05	1	645	91	316	554	9.47	14.11	22.36	17.30
r06	2	674	136	324	538	13.63	20.18	29.57	23.99
r07	3	627	383	168	244	48.18	61.08	69.51	65.02
r08	2	651	629	16	22	94.30	96.62	97.52	97.07
r09	2	657	382	225	275	43.31	58.14	62.93	60.44
r10	2	637	495	133	142	64.29	77.71	78.82	78.26
r11	2	705	196	341	509	18.74	27.80	36.50	31.56
r12	2	685	96	306	589	9.69	14.01	23.88	17.66

TABLE 2. Statistical evaluation of the detection of fQRS complexes obtained by the ICA-EMD and ICA-EMD-WT methods that was tested on signals from the ADFECGDB database.

Recordings	Combination of electrodes	ICA-EMD				ICA-EMD-WT			
		ACC (%)	Se (%)	PPV (%)	F1 (%)	ACC (%)	Se (%)	PPV (%)	F1 (%)
r01	1, 3, 4	95.71	97.05	98.58	97.81	97.98	98.14	99.84	98.98
r02	1, 2, 3, 4	96.10	97.12	98.92	98.01	92.46	94.70	97.50	96.08
r03	2, 4	9.65	14.18	23.21	17.60	9.87	14.47	23.68	17.96
r04	1, 4	17.92	26.42	35.76	30.39	28.72	40.66	49.42	44.61
r05	1, 4	95.10	96.28	98.73	97.49	81.21	87.13	92.28	89.63
r06	1, 2, 3, 4	9.76	14.24	23.65	17.78	13.61	20.62	28.60	23.96
r07	1, 4	18.59	26.00	39.47	31.35	31.96	43.22	55.08	48.43
r08	1, 4	95.73	96.31	99.37	97.82	97.70	97.70	100.00	98.84
r09	1, 2, 4	89.09	90.72	98.03	94.23	84.27	88.89	94.19	91.46
r10	1, 2, 3, 4	22.46	32.65	41.85	36.68	55.64	66.56	77.23	71.50
r11	1, 2, 3, 4	18.93	27.23	38.32	31.84	19.57	29.65	36.54	32.74
r12	1, 2, 3, 4	9.61	13.72	24.29	17.54	9.97	14.89	23.18	18.13

80% was received for r09 recording. According to the PPV parameter, accuracy of over 95% was achieved for r01, r02, r05, r08 and r09 recordings. According to the F1 parameter, accuracy of over 95% was achieved for r01, r02, r05, and r08 recordings and accuracy of over 80% was received for r09 recording.

As for the ICA-EMD-WT method, it is possible to determine that accuracy of over 95% for r01 and r08 recordings and accuracy of over 80% for r02, r05 and r09 recordings was achieved by the ACC parameter. According to the Se parameter, accuracy of over 95% was achieved for r01 and r08 recordings and accuracy of over 80% was received for r02, r05 and r09 recordings. According to the PPV parameter, accuracy of over 95% was achieved for r01, r02 and r08 recordings and accuracy of over 80% was received for r05 and r09 recordings. According to the F1 parameter, accuracy of over 95% was achieved for r01, r02 and r08 recordings and accuracy of over 80% was received for r05 and r09 recordings. For other recordings, relatively low precision values were achieved and the method was not very effective for these recordings.

The last method tested was the ICA-RLS-EMD, which aims to remove the residual mECG and to improve the fECG by proper setting of the filter order and by appropriately selecting IMFs, the sum of which will contribute to the generation of an improved fECG. As this method achieved the best results on real data from the ADFECGDB database, it was also tested on data from the Challenge 2013 database. The results achieved by the ICA-RLS-EMD method are recorded in Tab. 3 and Tab. 4. Furthermore, fHR traces and Bland-Altman plots were illustrated for the results obtained by the ICA-RLS-EMD method.

According to Tab. 3, as for the ICA-RLS-EMD method, it is possible to determine that accuracy of over 95% for r01, r02, r03, r05, r08 and r09 recordings and accuracy of over 80% for r06, r10 and r12 recordings was achieved by the ACC parameter. According to the Se parameter, accuracy of over 95% was achieved for r01, r02, r03, r05, r08, r09 and r10 recordings and accuracy of over 80% was received for r06 and r12 recordings. According to the PPV parameter, accuracy of over 95% was achieved for r01, r02, r03, r05, r06, r08, r09 and r12 recordings and accuracy of over 80% was received for r07 and r10 recordings. According to the F1 parameter, accuracy of over 95% was achieved for r01, r02, r03, r05, r08, r09 and r10 recordings and accuracy of over 80% was received for r06 and r12 recordings. For other recordings, relatively low precision values were achieved and the method was not very effective for these recordings. The lowest number of FP and FN values was achieved in r05 and r08 recordings. For r05 and r09 recordings, the method did not

TABLE 3. Statistical evaluation of the detection of fQRS complexes obtained by the ICA-RLS-EMD method that was tested on signals from the ADFECGDB database.

Recordings	Combination of electrodes	Filter order	n	TP	FP	FN	ACC (%)	Se (%)	PPV (%)	F1 (%)
r01	1, 3, 4	2	644	642	1	2	99.53	99.69	99.84	99.76
r02	1, 2, 3, 4	16	660	658	1	2	99.55	99.70	99.85	99.77
r03	2, 4	86	684	677	2	7	98.69	98.98	99.71	99.34
r04	1, 4	46	632	379	102	253	51.63	59.97	78.79	68.10
r05	1, 4	16	645	643	0	2	99.69	99.69	100.00	99.84
r06	1, 2, 3, 4	98	674	630	27	44	89.87	93.47	95.89	94.66
r07	1, 4	46	627	438	72	189	62.66	69.86	85.88	77.05
r08	1, 4	30	651	650	1	1	99.69	99.85	99.85	99.85
r09	1, 2, 4	16	657	652	0	5	99.24	99.24	100.00	99.62
r10	1, 2, 3, 4	52	637	617	33	20	92.09	96.86	94.92	95.88
r11	1, 2, 3, 4	80	705	343	211	362	37.45	48.65	61.91	54.48
r12	1, 2, 3, 4	100	685	616	26	69	86.64	89.93	95.95	92.84

TABLE 4. Statistical evaluation of the detection of fQRS complexes obtained by the ICA-RLS-EMD method that was tested on signals from the Physionet Challenge 2013 database.

Recordings	Combination of electrodes	Filter order	n	TP	FP	FN	ACC (%)	Se (%)	PPV (%)	F1 (%)
a01	1, 2, 3	10	145	134	7	11	88.16	92.41	95.04	93.71
a02	1, 2, 4	2	160	27	36	133	13.78	16.88	42.86	24.22
a03	1, 4	100	128	116	5	12	87.22	90.63	95.87	93.18
a04	1, 2	64	129	129	1	0	99.23	100.00	99.23	99.61
a05	1,3	32	129	129	0	0	100.00	100.00	100.00	100.00
a06	2, 4	24	160	76	21	84	41.99	47.50	78.35	59.14
a07	1, 2, 3, 4	66	130	55	57	75	29.41	42.31	49.11	45.46
a08	1, 4	100	128	128	0	0	100.00	100.00	100.00	100.00
a09	1, 4	94	130	32	72	98	15.84	24.62	30.77	27.35
a10	2, 4	98	175	118	14	57	62.43	67.43	89.39	76.87
a11	1, 4	24	140	35	23	105	21.47	25.00	60.34	35.35
a12	1,3, 4	14	138	130	4	8	91.55	94.20	97.01	95.58
a13	2, 4	36	126	95	6	31	71.97	75.40	94.06	83.70
a14	1, 2, 3, 4	10	123	105	8	18	80.15	85.37	92.92	88.99
a15	1, 4	94	134	133	0	1	99.25	99.25	100.00	99.62
a16	1, 4	40	130	32	64	98	16.49	24.62	33.33	28.32
a17	1, 4	100	132	132	0	0	100.00	100.00	100.00	100.00
a18	1, 2, 3, 4	34	150	18	82	132	7.76	12.00	18.00	14.40
a19	3, 4	42	127	102	10	25	74.45	80.31	91.07	85.35
a20	1, 4	96	131	78	14	53	53.79	59.54	84.78	69.95
a21	2, 3, 4	4	145	89	21	56	53.61	61.38	80.91	69.80
a22	1, 4	32	126	126	0	0	100.00	100.00	100.00	100.00
a23	1, 3	36	126	67	31	59	42.68	53.17	68.37	42.68
a24	1, 3	50	123	113	8	10	86.26	91.87	93.39	92.62
a25	2, 3	94	125	112	5	13	86.15	89.60	95.73	92.56

detect any FP value, so 100% accuracy was achieved with the PPV parameter.

To illustrate the differences in the extraction outcomes, we decided to plot the examples of individual input signals. Figure 9 shows the examples of the abdominal signals from the tested database along with the signals estimated using ICA algorithm that were used as the reference and primary inputs (mECG* and aECG, respectively) to the adaptive algorithms.

We selected 3 recordings for the ilustration - recordings r01, r04, and r07, where recording r01 is the example of recording with excellent results (F1>95%) in the fECG extraction whereas recordings r04 and r07 are the recordings with the poor results in the fECG extraction (F1<80%). The notable differences between these examples are the quality of the aECG signals and the ratio between the maternal and fetal component in those signals. The performance of the adaptive algorithm strongly correlates with the quality of its inputs, especially with the reference signal (mECG*). Some of the mECG* ICA estimates were of a poor quality (i.e. included noise or the fECG residua) which led to decreased accuracy of the fECG extraction.

Additionally, the morphology of the mECG* reference signal should correspond to the shape of the maternal component in aECG*. However, in the case of recordings r04 and r07, the maternal components in both aECG* signals are bipolar whereas the reference mECG* signal has positive polarity. This is caused by the difference in the corresponding abdominal inputs. The electrode deployment and data acquisition quality are of a great importance to achieve accurate fECG

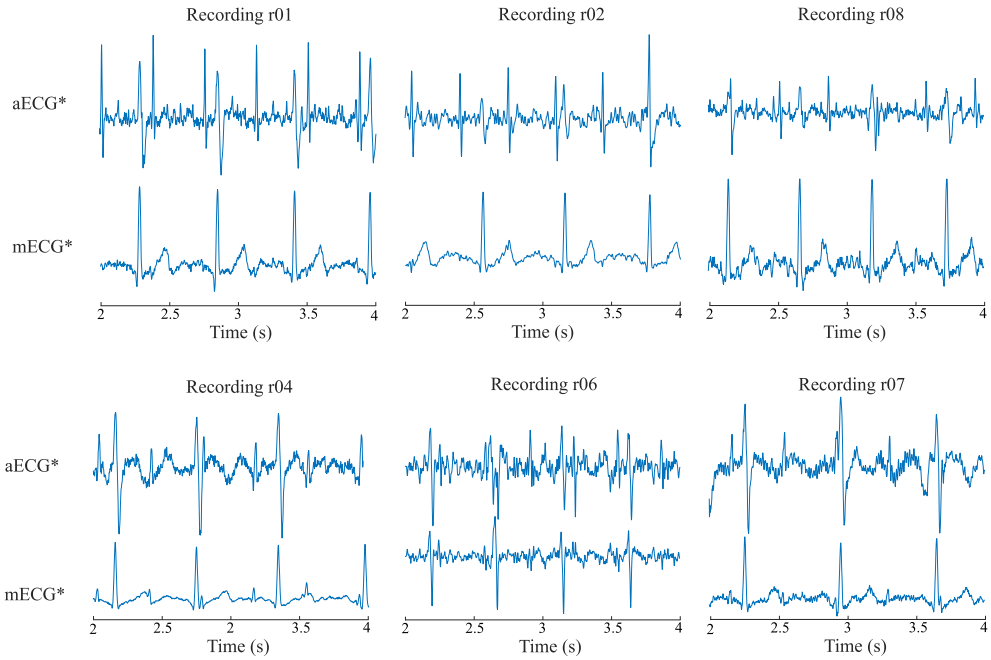

FIGURE 9. Examples of the abdominal ECG signals and estimated maternal (mECG*) and abdominal signals (aECG*) used for the experiments. Top row from left to right: Example of the input abdominal and direct ECG recordings r01, r04, and r07; Bottom row from left to right: examples of estimated mECG* and aECG* for recordings r01, r04, and r07.

TABLE 5. Mean values μ and values of $\pm 1.96\sigma$ determined for all hybrid methods.

Recordings	ICA-EMD		ICA-EMD-WT		EMD-WT		ICA-RLS-EMD	
	μ (bpm)	$\pm 1.96\sigma$ (bpm)	μ (bpm)	$\pm 1.96\sigma$ (bpm)	μ (bpm)	$\pm 1.96\sigma$ (bpm)	μ (bpm)	$\pm 1.96\sigma$ (bpm)
r01	-0.75	6.09	-0.92	-0.92	-7.73	20.49	-0.25	5.39
r02	-0.57	9.01	-6.10	-6.10	-10.88	20.98	-0.22	7.63
r03	-50.89	24.92	-50.71	-50.71	-52.09	21.67	-0.26	2.91
r04	-17.52	21.38	-8.65	-8.65	-22.93	22.18	-12.38	20.54
r05	-1.01	5.37	-46.05	-46.05	-7.00	15.65	-0.13	4.13
r06	-48.91	19.44	-37.71	-37.71	-46.15	21.71	-1.15	5.62
r07	-23.06	17.69	-4.24	-4.24	-33.88	19.08	-8.92	13.97
r08	-2.13	8.61	-0.23	-0.23	-5.24	15.73	-0.26	7.12
r09	-4.10	10.74	1.28	1.28	-10.18	17.08	-0.48	3.60
r10	-20.02	24.22	0.14	0.14	-34.33	27.25	-0.32	8.73
r11	-32.91	27.30	-31.77	-31.77	-47.05	44.30	-19.00	27.70
r12	-54.61	18.85	-51.06	-51.06	-47.48	25.01	-3.71	12.94

extraction. Therefore, further research should be focused on the effects of the electrode placement and system configuration and their effects on the signal quality along with other factors such as fetal position or gestation age.

According to Tab. 4, as for the ICA-RLS-EMD method, it is possible to determine that accuracy of over 95% for a04, a05, a08, a15, a17, and a22 recordings and accuracy of over 80% for a01, a03, a12, a14, a24 and a25 recordings was achieved by the ACC parameter. According to the Se parameter, accuracy of over 95% was achieved for a04, a05, a08, a15, a17, and a22 recordings and accuracy of over 80% was received for a01, a03, a12, a14, a19, a24 and a25 recordings. According to the Se parameter, accuracy of over 95% was achieved for a01, a03, a04, a05, a08, a12, a15, a17, a22 and a25 recordings and accuracy of over 80% was received for a10, a13, a14, a19, a20, a21 and a24 recordings. According to the F1 parameter, accuracy of over 95% was achieved for a04, a05, a08, a12, a15, a17, and a22 recordings and accuracy of over 80% was received for a01, a03, a13, a14, a19, a24 and a25 recordings. For other recordings, relatively low precision values were achieved and the method was not very effective for these recordings. The lowest number of FP and FN values was achieved in a05, a08, a17 and a22 recordings. For these recordings, the method did not detect any FP or FN values, so 100% accuracy was achieved with all the parameters (ACC, Se, PPV and F1).

Similarly as in the case of the previous recordings, we selected examples of recordings with various levels of extraction efficacy for the explanation. Figure 10 shows examples of in total 8 recordings, for 4 of them

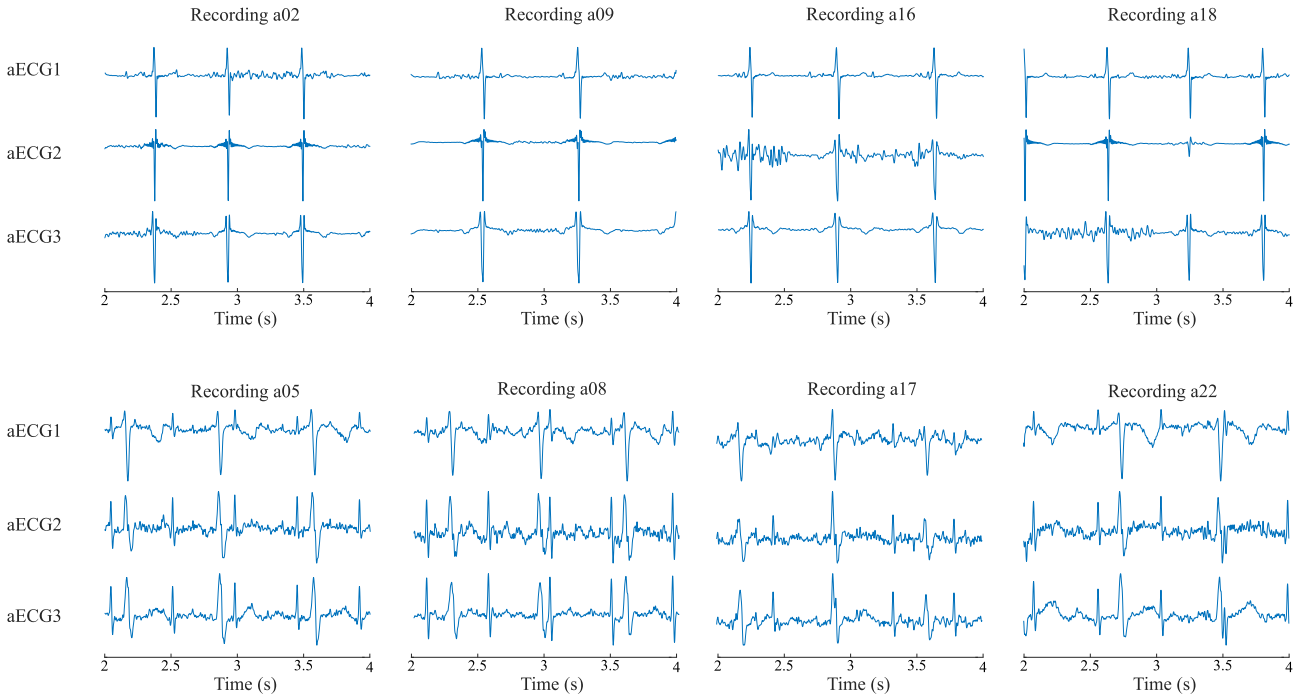

FIGURE 10. Examples of the abdominal ECG signals used for the experiments. Top row from left to right: Example of the 3 selected input aECG signals from recordings a02, a09, a16, and a18; Bottom row from left to right: Example of the 3 selected input aECG signals from recordings a05, a08, a17, and a22.

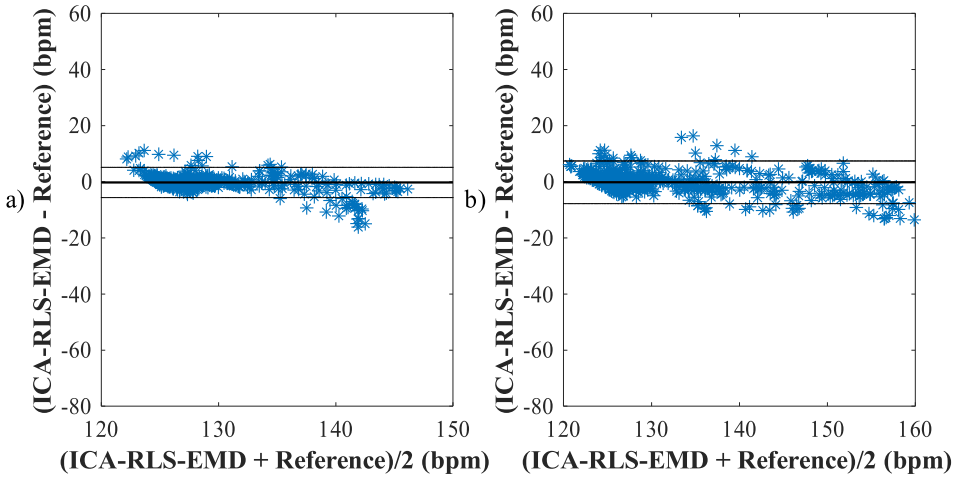

FIGURE 11. Representation of the ability to detect fQRS complexes based on the Bland-Altman plot using the ICA-RLS-EMD method, a) for r01 recording and b) for r02 recording.

(r02, a09, a16, and a18) the results were poor (F1<50%) while other recordings (a05, a08, a17, and a22), the results were excellent (F1=100%). Again, the difference between the quality of the input signals was remarkable, especially in terms of the ratio between maternal and fetal component magnitude. It must be noted that the fetal component in the recordings r02, a09, a16, and a18 is hardly notable by the naked eye and thus the fECG extraction is extremely difficult. Also, there is significant amount of noise present which also significantly influences the performance of the adaptive algorithm.

B. BLAND-ALTMAN PLOTS

Bland-Altman plots are also used to graphically assess the accuracy of the fHR detection. This study compares fHR measurement results determined by the method and determined using the annotation. Figure 11, Fig. 12, and Fig. 13 show Bland-Altman plots for the properly functioning ICA-RLS-EMD method.

First, the differences of the two measurements are determined and the mean value of these differences is specified, then the limits of agreement (LoA) are set as the mean value of $\mu \pm 1.96\sigma$ (where σ is the standard deviation). This is an

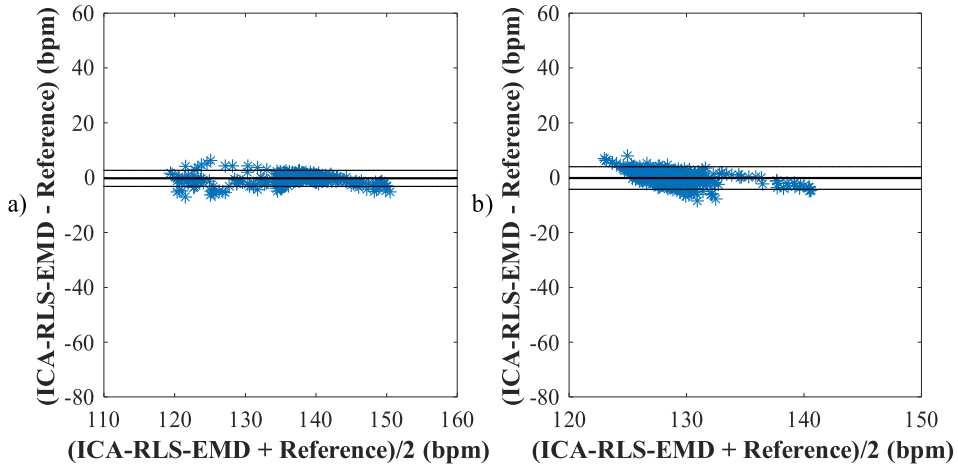

FIGURE 12. Representation of the ability to detect fQRS complexes based on the Bland-Altman plot using the ICA-RLS-EMD method, a) for r03 recording and b) for r05 recording.

estimate of the interval at which 95% of the difference values can be expected [35]. The result is considered acceptable if the values of the determined differences lie within this limit, otherwise the value is indicated as an error [17]. The values μ and $\pm 1.96\sigma$ for all methods are recorded in Tab. 5.

In graphical form, the vertical axis denotes the values of the difference vector, which are determined as *method* − *reference*, and the horizontal axis denotes the values of the difference average vector, which are determined as $\frac{method + reference}{2}$, where *reference* denotes the fHR values of the annotation and method denotes the fHR values of the method tested. The depiction itself includes three axes, the upper one determines the limit of agreement the mean value is $+1.96\sigma$, the middle value determines the mean value of the differences, and the lower one determines the limit of agreement of the mean value of -1.96σ [17].

The data can be interpreted as follows: the closer to zero the μ value and $\pm 1.96\sigma$ are, the smaller the difference between the extracted and reference fHR values is. As for the ICA-EMD method, low values of μ and $\pm 1.96\sigma$ were obtained for r01, r02, r05, and r08 recordings. As for the ICA-EMD-WT method, low μ values were obtained for r01, r02, r05, r08, and r09 recordings, and it can be stated that the methods are effective for these recordings. As for the EMD-WT method, low μ values were obtained for r01, r08, r09, and r10 recordings, and it can be stated that the methods are effective for these recordings, but high $\pm 1.96\sigma$ values were achieved for r09 and r10 recordings, so this statement is invalid for these recordings. As for the ICA-RLS-EMD method, low μ values were obtained for r01, r02, r03, r05, r06, r08, r09, and r10 recordings, thus, the method is effective for all of these recordings.

C. FETAL HEART RATE TRACES

Depiction of fHR traces is achieved by determining the current fHR value between the individual R-peaks in the entire recording. First, it is necessary to detect the R-peaks and to determine the RR intervals. From these intervals, it is then necessary to determine the current heart rates between the individual R-peaks. The position of the R-peaks is specified using a precise detector that utilizes a complex WT to find all local minima and maxima. Subsequently, a moving average is found for the values obtained by the method. The moving average is a time series created using the average of several sequence values of another time series. Based on the moving averages, fHR traces were created and compared with annotations where R-peaks are determined by experts. The graphical representation is based on FIGO classification [38]. The interval of physiological fHR values is marked in white and indicates values in the range from 110 to 150 bpm. The area marked in yellow is an area with an increased risk of hypoxia, i.e. the fHR ranges from 90 to 110 bpm and from 150 to 180 bpm. Pink indicates an area with a high risk of hypoxia, i.e. the fHR values below 80 bpm and above 180 bpm [15]. Figure 14 illustrates the fHR traces obtained by the ICA-RLS-EMD method, according to which it can be stated that the method works correctly for r01, r02, r03, r05, r06, r08, r09, and r10 recordings because the method curves follow the annotation trend. For recordings r04, r07, r11, and r12, the deviation of the fHR trace, determined using the estimated fECG signal, from the reference fHR trace can be seen, which means that the method was not very effective for these recordings.

D. RESULTS COMPARISON

Finally, this subsection provides the comparison of the results obtained in this study with the extraction methods proposed by other authors. It is important to note that such comparison is difficult since the dataset and the evaluation methods used vary among the articles on fECG extraction. For example, the authors in [7], [19] used a different database to test the methods or did not provide a database name, and thus comparison of the results is not possible. In addition, some

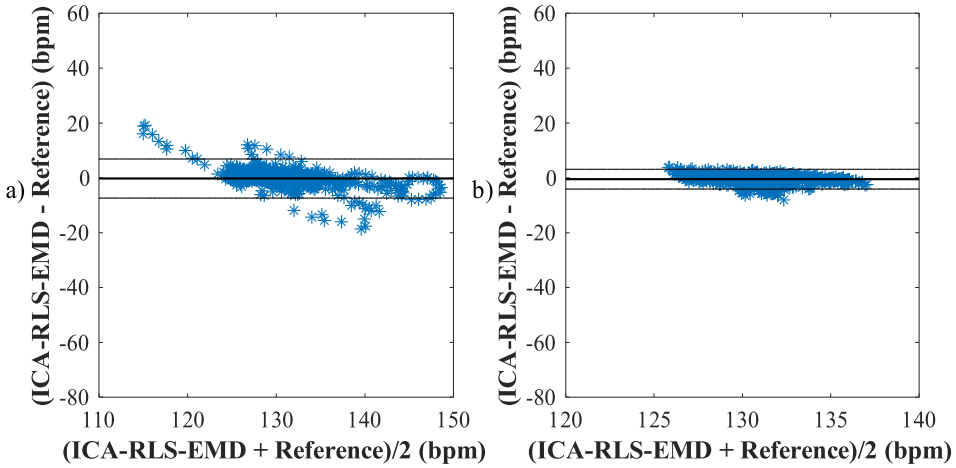

FIGURE 13. Representation of the ability to detect fQRS complexes based on the Bland-Altman plot using the ICA-RLS-EMD method, a) for r08 recording and b) for r09 recording.

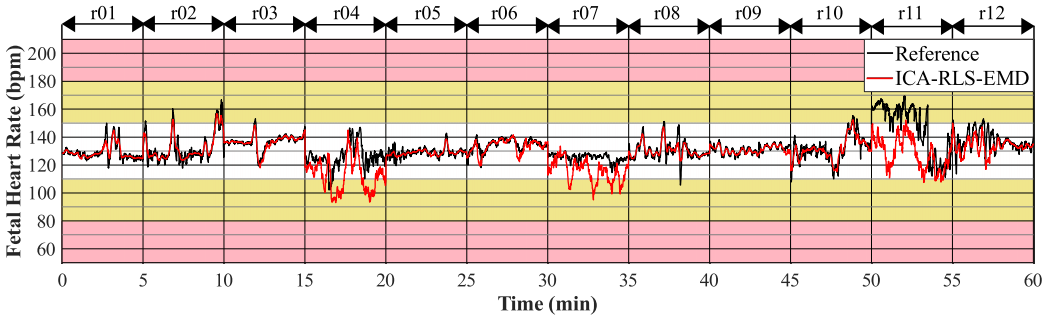

FIGURE 14. Depiction of fHR traces for all recordings and their annotations from the ADFECGDB database, extracted using the ICA-RLS-EMD method.

studies [11], [25] use other statistical parameters to evaluate methods. The authors in [11] tested the methods on the same dataset but used correlation coefficients (R) to assess the similarity of the scalp fECG signal with the estimated one. Moreover, some studies, such as [23], [29] provide no statistical evaluation and present only the examples of the extracted fECG signals.

Finally, authors in [13], [22] used the same database and the same evaluation parameters to test their methods. In [22], the authors combined the EMD-based algorithms (EMD, EEMD, and CEEMD) with the correlation and match filtering and tested this extraction system on 4 ADFECGDB records, which were not further specified. In addition, the methods were probably only tested on limited samples of the signals, as the authors report 100% accuracy of the method but at the same time there were only about 20 TP values detected for all of the signals (compared to 600–700 TP values according to the annotations). Such a comparison is thus not very relevant.

In [13], a method based on wavelet transform was used for signal denoising and a clustering-based technique for fQRS complex detection. The authors performed experiments on r01, r04, r07, r08, and r10 records only. Compared to the study presented in [13], the ICA-RLS-EMD method presented herein achieved better results for r01 and r08 recordings, while for r04, r07, and r10 it was outperformed. However, this comparison contained only a fraction of the dataset and thus such comparison is not very informative.

In our previous study [15], we introduced two different hybrid extraction systems (ICA-ANFIS-WT and ICA-RLS-WT). The same databases (ADFECGDB and Physionet Challenge 2013) and evaluation parameters (ACC, Se, PPV, and F1) were used to assess the extraction system performance. The results showed that the ICA-RLS-WT method outperforms the ICA-ANFIS-WT system. Although the performance of those methods was high for the fHR monitoring, these methods are not suitable for further morphological analysis. This is due to WT method, which was used for smoothing of the estimated fECG signal causing deformation of the fECG morphology. Thus, this approach could not be utilized in e.g. non-invasive ST analysis. This drawback can be overcome by replacing the WT by EMD method. The ICA-RLS-EMD system reached comparable results with ICA-RLS-WT system in terms of fHR monitoring, while keeping the morphology of the fECG waveform unaffected.

V. DISCUSSION

The results presented in the previous chapters show that a hybrid system combining EMD with other methods is

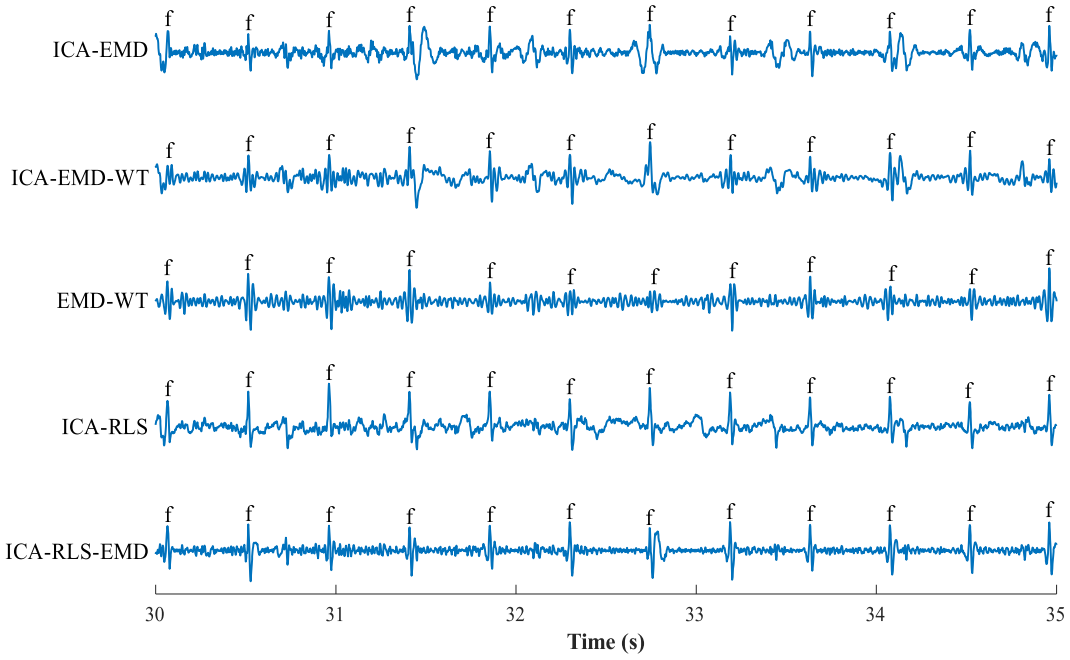

FIGURE 15. Examples of signals extracted by all the hybrid systems tested for r08 recording.

capable of determining fHR with high accuracy. Each of these methods has its advantages and limitations, as shown by the extraction examples in Fig. 15. The ICA-EMD combination has a limited ability to suppress the maternal component, which cannot be reliably removed even by the subsequent application of the wavelet transform (see the example of ICA-EMD-WT extraction). This leads to an increase in false positive peaks occurrence and, thus, to a decrease in filtration quality expressed by ACC or F1. In contrast, when EMD is combined with WT, the maternal component is more effectively eliminated, but the fetal component is also significantly suppressed (see the example of EMD-WT extraction). This leads, on the contrary, to an increased number of false negative peak detection and, thus, also to a decrease in extraction accuracy expressed by the objective parameters of ACC or F1.

The best results were achieved by a hybrid system containing adaptive filtering using the RLS algorithm. It is important to note that the RLS algorithm cannot be used alone if only abdominal leads are available. For this reason, it is advantageous to use it in combination with ICA that is capable of providing both reference and primary input to the adaptive system. As such, the combination is able to provide an extracted fECG signal in high quality (see the example of ICA-RLS extraction). The subsequent application of the EMD method causes almost complete elimination of the maternal component, thus increasing the overall efficiency of the system (see the example of ICA-RLS-EMD extraction).

The aforementioned demonstrates a comparison of fHR traces obtained by the ICA-RLS-EMD method with the fHR trace obtained by means of references for r01 recording, see Fig. 16. Reference was obtained using fetal scalp electrode (invasive fECG monitoring). Performance comparison was done according to reference annotations containing markers that accurately indicate the location of R-peaks. These R-peaks were determined by an on-line analysis using the KOMPOREL system and, subsequently, the placement of the markers was verified by a group of cardiologists. To illustrate the extraction efficiency using a specific system, we also present examples of extracted, abdominal and reference signals for selected fHR traces. These samples correspond to sections of fHR trace where successful filtering was achieved (the estimated fHR trace coincides with the reference one) as well as to sections where the filtering was not successful (the fHR traces differ from each other). Minor deviations of the estimated fHR trace occurred only at places where the maternal component had significantly higher voltage level than the fetal component (examples d), e) and f)). However, these slight deviations are not significant enough to affect the final diagnosis.

Figure 17 shows a comparison of fHR traces obtained by the ICA-RLS-EMD method and the annotation for r12 recording. Again, we also present examples of extracted, abdominal and reference signals for the selected parts of the fHR trace. The three examples a), b) and c) of extracted, abdominal and reference signals correspond to sections of fHR trace where successful filtering was achieved. These are parts of the abdominal signal where the maternal component is dominant, but the fetal component is of sufficient voltage level. The remaining examples d), e), and f) then show sections where the estimated fHR curve deviates significantly

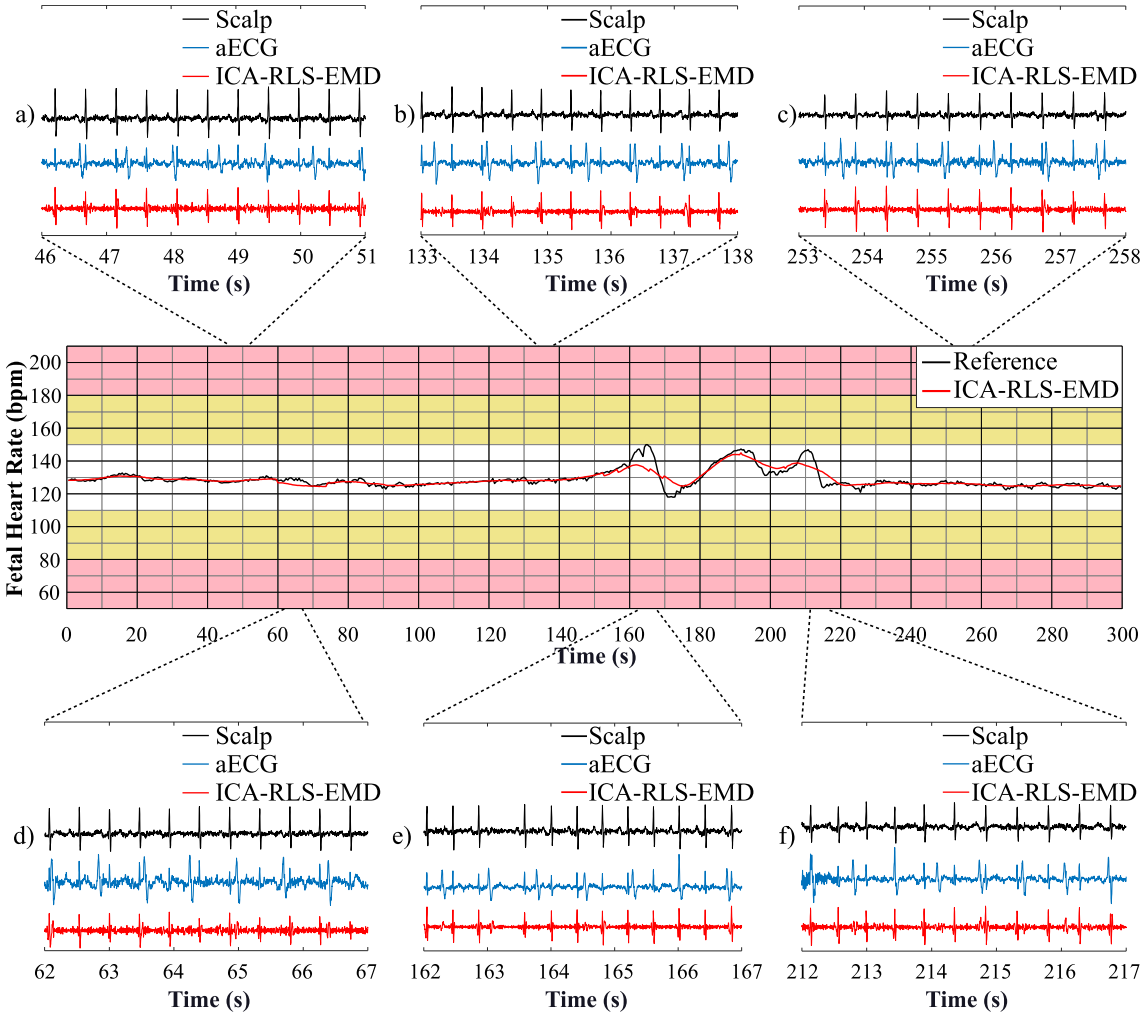

FIGURE 16. Depiction of fHR traces obtained using the ICA-RLS-EMD method and the annotation for r01 recording. Plots a), b) and c) show sections where the method worked correctly and plots d), e) and f) show sections where the method curve deviated slightly from the annotation curve.

from the reference curve. These parts of the abdominal signal also contain the dominant maternal component and the fetal component is at a very low level, but, moreover, there is noise in the signal that caused a reducing of the fECG extraction quality. The results of such extraction may lead to a false positive diagnosis of fetal hypoxia.

Based on the quantitative and qualitative results presented above, the ICA-RLS-EMD method is the most suitable hybrid method from the methods tested. As for the ADFECGDB database, it worked in 9 out of 12 recordings, reaching an average value of ACC $>$ 84%, Se $>$ 87%, PPV $>$ 92%, F1 $>$ 90%. As for the ICA-EMD and ICA-EMD-WT methods, ACC $>$ 80% in 5 out of 12 recordings and, as for the EMD-WT method, ACC $>$ 80% in only 2 out of 12 recordings when tested on the ADFECGDB database.

The ICA-RLS-EMD method was able to minimize the residues of the mECG component without significantly distorting the shape of the fQRS complexes. As for the WT methods, fQRS complexes were deformed by wavelets application, which is not an obstacle for determining the fHR, which is the primary goal of this study. Nevertheless, it should be noted that, in more advanced studies, this deformation would hinder the analysis of the ST segment morphology and the QT interval length.

One of the challenges that the future research should focus on is the optimal setup of the individual algorithms, especially the RLS algorithm, with an emphasis on preserving the morphology in terms of the ST segment analysis or the QT interval analysis. This could be enable introducing a non-invasive variant of the clinically used STAN (i.e. NI-STAN) diagnostic method. In combination with the classical fHR monitoring, this method would be able to increase the accuracy of the early diagnosis of fetal hypoxia, thereby reducing the number of unnecessary caesarean sections [39]. Furthermore, it will be necessary to test the systems on other databases, but, unfortunately, there is an acute shortage of them at present. Therefore, it is necessary to create a comprehensive database that complies with the standards regarding, for example, uniform sampling frequency, sufficient length and number of records and contains variations in the fetal position or the

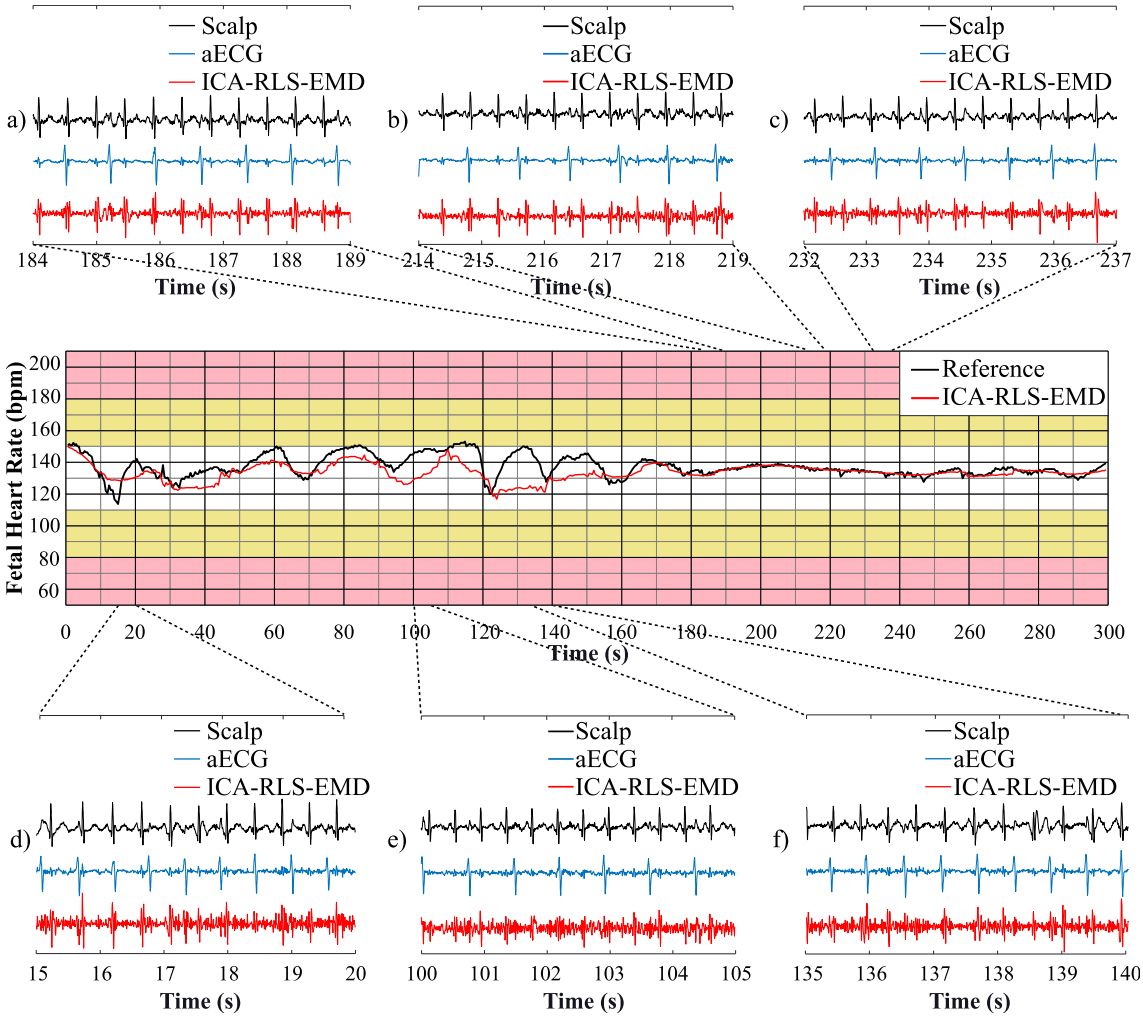

FIGURE 17. Depiction of fHR traces obtained using the ICA-RLS-EMD method and the annotation for r12 recording. Plots a), b) and c) show sections where the method worked correctly and plots d), e) and f) show sections where the method curve deviated significantly from the annotation curve.

pregnancy stage. This is also related to the need to unify the electrode deployment of the multi-channel system, which varies among different studies and commercial devices [40]. This would be of great importance for the antenatal monitoring where this system could help to detect various cardiovascular defects based on the changes in the morphology of the fECG waveform.

VI. CONCLUSION

This study examined the effectiveness of hybrid methods utilizing EMD, namely ICA-EMD, ICA-EMD-WT, EMD-WT, and ICA-RLS-EMD extraction systems. The tests conducted on two databases (ADFECGDB and PhysioNet Challenge 2013) have shown that combining two or more methods increases the efficiency of a specific extraction system. The evaluation of the hybrid systems was based on their ability to provide accurate information about the fetal heart rate. The statistical evaluation was based on evaluation by objective parameters, i.e. ACC, Se, PPV, and F1. The best results were achieved by the ICA-RLS-EMD method, with ACC $>$ 80% in 9 out of 12 recordings and average values of ACC $>$ 84%, Se $>$ 87%, PPV $>$ 92%, F1 $>$ 90%. When tested on the Physionet Challenge 2013 database, ACC $>$ 80% was achieved at 12 out of 25 recordings with an average value of ACC $>$ 64%, Se $>$ 69%, PPV $>$ 79%, F1 $>$ 72%. In the future research, this study will be extended with an analysis of the ST segment and the QT interval in the extracted signals. This can enable a non-invasive variant of the currently available morphological analysis of the fECG signal acquired by the invasive scalp electrode.

ETHICS STATEMENT

The study protocol was approved by the Ethical Committee of the Silesian Medical University, Katowice, Poland (NN-013-345/02). Subjects read the approved consent form and gave written informed consent to participate in the study.

REFERENCES

[1] E. H. Hon and E. J. Quilligan, "The classification of FHR, II revised ed, Working classification," *Conn Med*, vol. 31, no. 11, pp. 779–784, Nov. 1967.

[2] C. N. Smyth and J. L. Farrow, "Present place in obstetrics for foetal phonocardiography and electrocardiography," *Brit. Med. J.*, vol. 2, no. 5103, pp. 1005–1009, Oct. 1958. [Online]. Available: http://www.bmj.com/cgi/doi/10.1136/bmj.2.5103.1005

[3] W. R. Cohen and B. Hayes-Gill, "Influence of maternal body mass index on accuracy and reliability of external fetal monitoring techniques," *Acta Obstetricia et Gynecologica Scandinavica*, vol. 93, no. 6, pp. 590–595, Apr. 2016. [Online]. Available: http://doi.wiley.com/10.1111/aogs.12387

[4] T. Y. Euliano, M. T. Nguyen, S. Darmanjian, S. P. McGorray, N. Euliano, A. Onkala, and A. R. Gregg, "Monitoring uterine activity during labor: A comparison of 3 methods," *Amer. J. Obstetrics Gynecology*, vol. 208, no. 1, pp. 66.e1–66.e6, Jan. 2013. [Online]. Available: https://linkinghub.elsevier.com/retrieve/pii/S0002937812019734

[5] T. P. Sartwelle, "Electronic fetal monitoring: A bridge too far," *J. Legal Med.*, vol. 33, no. 3, pp. 313–379, Jul. 2012. [Online]. Available: http://www.tandfonline.com/doi/abs/10.1080/01947648.2012.714321

[6] J. Spilka, V. Chudácek, P. Janků, L. Hruban, M. Burša, M. Huptych, L. Zach, and L. Lhotská, "Analysis of obstetricians' decision making on CTG recordings," *J. Biomed. Informat.*, vol. 51, pp. 72–79, Oct. 2014. [Online]. Available: https://linkinghub.elsevier.com/retrieve/pii/S1532046414000951

[7] L. de Lathauwer, B. de Moor, and J. Vandewalle, "Fetal electrocardiogram extraction by blind source subspace separation," *IEEE Trans. Biomed. Eng.*, vol. 47, no. 5, pp. 567–572, May 2000.

[8] D. Callaerts, "Signal separation methods based on singular value decomposition and their application to the real-time extraction of the fetal electrocardiogram from cutaneous recordings," Tech. Rep., 1989. [Online]. Available: https://limo.libis.be/primo-explore/fulldisplay?docid=LIRIAS1692001&context=L&vid=Lirias&search_scope=Lirias&tab=default_tab&lang=en_US&fromSitemap=1

[9] R. Martinek, R. Kahankova, H. Nazeran, J. Konecny, J. Jezewski, P. Janku, P. Bilik, J. Zidek, J. Nedoma, and M. Fajkus, "Non-invasive fetal monitoring: A maternal surface ECG electrode placement-based novel approach for optimization of adaptive filter control parameters using the LMS and RLS algorithms," *Sensors*, vol. 17, no. 5, p. 1154, May 2017. [Online]. Available: http://www.mdpi.com/1424-8220/17/5/1154

[10] J. Behar, J. Oster, and G. D. Clifford, "Non-Invasive FECG Extraction from a Set of Abdominal Sensors," in *Computing in Cardiology*. Piscataway, NJ, USA: Institute of Electrical and Electronics Engineers, 2013, pp. 297–300.

[11] G. Liu and Y. Luan, "An adaptive integrated algorithm for noninvasive fetal ECG separation and noise reduction based on ICA-EEMD-WS," *Med. Biol. Eng. Comput.*, vol. 53, no. 11, pp. 1113–1127, Nov. 2015. [Online]. Available: http://link.springer.com/10.1007/s11517-015-1389-1

[12] N. E. Huang, Z. Shen, S. R. Long, M. C. Wu, H. H. Shih, Q. Zheng, N.-C. Yen, C. C. Tung, and H. H. Liu, "The empirical mode decomposition and the Hilbert spectrum for nonlinear and non-stationary time series analysis," *Proc. Roy. Soc. London. Ser. A: Math., Phys. Eng. Sci.*, vol. 454, no. 1971, pp. 903–995, Mar. 1998. .[Online]. Available: https://royalsocietypublishing.org/doi/10.1098/rspa.1998.0193

[13] E. Castillo, D. P. Morales, A. García, L. Parrilla, V. U. Ruiz, and J. A. Álvarez-Bermejo, "A clustering-based method for single-channel fetal heart rate monitoring," *PLoS ONE*, vol. 13, no. 6, Jun. 2018, Art. no. e0199308. [Online]. Available: https://dx.plos.org/10.1371/journal.pone.0199308

[14] D. Panigrahy and P. K. Sahu, "Extraction of fetal ECG signal by an improved method using extended Kalman smoother framework from single channel abdominal ECG signal," *Australas. Phys. Eng. Sci. Med.*, vol. 40, no. 1, pp. 191–207, Mar. 2017. [Online]. Available: http://link.springer.com/10.1007/s13246-017-0527-5

[15] R. Jaros, R. Martinek, R. Kahankova, and J. Koziorek, "Novel hybrid extraction systems for fetal heart rate variability monitoring based on non-invasive fetal electrocardiogram," *IEEE Access*, vol. 7, pp. 131758–131784, 2019. [Online]. Available: https://ieeexplore.ieee.org/document/8790705/

[16] R. Jaros, R. Martinek, and R. Kahankova, "Non-adaptive methods for fetal ECG signal processing: A review and appraisal," *Sensors*, vol. 18, no. 11, p. 3648, Oct. 2018. [Online]. Available: http://www.mdpi.com/1424-8220/18/11/3648

[17] R. Martinek, R. Kahankova, J. Jezewski, R. Jaros, J. Mohylova, M. Fajkus, J. Nedoma, P. Janku, and H. Nazeran, "Comparative effectiveness of ICA and PCA in extraction of fetal ECG from abdominal signals: Toward non-invasive fetal monitoring," *Frontiers Physiol.*, vol. 9, p. 648, May 2018. [Online]. Available: https://www.frontiersin.org/article/10.3389/fphys.2018.00648/full

[18] P. M. Bentley and J. T. E. McDonnell, "Wavelet transforms: An introduction," *Electron. Commun. Eng. J.*, vol. 6, no. 4, pp. 175–186, Aug. 1994. [Online]. Available: https://digital-library.theiet.org/content/journals/10.1049/ecej_199404%01

[19] Y. Zeng, S. Liu, and J. Zhang, "Extraction of fetal ECG signal via adaptive noise cancellation approach," in *Proc. 2nd Int. Conf. Bioinf. Biomed. Eng.*, Shanghai, China, May 2008, pp. 2270–2273. [Online]. Available: http://ieeexplore.ieee.org/document/4535779/

[20] S. Pal and M. Mitra, "Empirical mode decomposition based ECG enhancement and QRS detection," *Comput. Biol. Med.*, vol. 42, no. 1, pp. 83–92, Jan. 2012. [Online]. Available: https://linkinghub.elsevier.com/retrieve/pii/S0010482511002083

[21] E. Izci, M. A. Ozdemir, R. Sadighzadeh, and A. Akan, "Arrhythmia detection on ECG signals by using empirical mode decomposition," in *Proc. Med. Technol. Nat. Congr. (TIPTEKNO)*, Magusa, Cyprus, Nov. 2018, pp. 1–4. [Online]. Available: https://ieeexplore.ieee.org/document/8597094/

[22] P. Ghobadi Azbari, M. Abdolghaffar, S. Mohaqeqi, M. Pooyan, A. Ahmadian, and N. Ghanbarzadeh Gashti, "A novel approach to the extraction of fetal electrocardiogram based on empirical mode decomposition and correlation analysis," *Australas. Phys. Eng. Sci. Med.*, vol. 40, no. 3, pp. 565–574, Sep. 2017. [Online]. Available: http://link.springer.com/10.1007/s13246-017-0560-4

[23] P. K. Ghosh and D. Poonia, "Comparison of some EMD based technique for baseline wander correction in fetal ECG signa," *Int. J. Comput. Appl.*, vol. 116, no. 15, pp. 48–52, Apr. 2015. [Online]. Available: http://research.ijcaonline.org/volume116/number15/pxc3902836.pdf

[24] J. M. Tanskanen and J. J. Viik, "Independent component analysis in ECG signal processing," in *Advances in Electrocardiograms-Methods and Analysis*. London, U.K.: IntechOpen, 2012.

[25] C. G. Raj, V. S. Harsha, B. S. Gowthami, and R. Sunitha, "Virtual instrumentation based fetal ECG extraction," *Procedia Comput. Sci.*, vol. 70, pp. 289–295, Jan. 2015. [Online]. Available: https://linkinghub.elsevier.com/retrieve/pii/S1877050915032573

[26] R. Sameni, C. Jutten, and M. B. Shamsollahi, "What ICA provides for ECG processing: Application to noninvasive fetal ECG extraction," in *Proc. IEEE Int. Symp. Signal Process. Inf. Technol.*, Vancouver, BC, Canada, Aug. 2006, pp. 656–661. [Online]. Available: https://ieeexplore.ieee.org/document/4042324/

[27] P. S. Addison, "Wavelet transforms and the ECG: A review," *Physiological Meas.*, vol. 26, no. 5, pp. R155–R199, Oct. 2005. [Online]. Available: http://stacks.iop.org/0967-3334/26/i=5/a=R01?key=crossref.dcbd88bb27589%993522323a5d05de0ee

[28] A. Godfrey, R. Conway, D. Meagher, and G. ÓLaighin, "Direct measurement of human movement by accelerometry," *Med. Eng. & Phys.*, vol. 30, no. 10, pp. 1364–1386, Dec. 2008. [Online]. Available: https://linkinghub.elsevier.com/retrieve/pii/S1350453308001653

[29] H. Hassanpour and A. Parsaei, "Fetal ECG extraction using wavelet transform," in *Proc. Int. Conf. Comput. Inteligence Modelling Control Automat. Int. Conf. Intell. Agents Web Technol. Int. Commerce (CIMCA)*. Sydney, NSW, Australia, Nov. 2006, p. 179. [Online]. Available: http://ieeexplore.ieee.org/document/4052801/

[30] R. Kahankova, R. Martinek, and P. Bilik, "Non-invasive Fetal ECG extraction from maternal abdominal ECG using LMS and RLS adaptive algorithms," in *Proc. 3rd Int. Afro-Eur. Conf. Ind. Advancement (AECIA)*, vol. 565. Cham, Switzerland: Springer, 2018, pp. 258–271. [Online]. Available: http://link.springer.com/10.1007/978-3-319-60834-1_27

[31] R. Kahankova, R. Martinek, and P. Bilik, "Fetal ECG extraction from abdominal ECG using RLS based adaptive algorithms," in *Proc. 18th Int. Carpathian Control Conf. (ICCC)*, Sinaia, Romania, May 2017, pp. 337–342. [Online]. Available: http://ieeexplore.ieee.org/document/7970422/

[32] A. C. Mugdha, F. S. Rawnaque, and M. U. Ahmed, "A study of recursive least squares (RLS) adaptive filter algorithm in noise removal from ECG signals," in *Proc. Int. Conf. Informat., Electron. Vis. (ICIEV)*, Fukuoka, Japan, Jun. 2015, pp. 1–6. [Online]. Available: http://ieeexplore.ieee.org/document/7333998/
[33] L. Billeci and M. Varanini, "A combined independent source separation and quality index optimization method for fetal ECG extraction from abdominal maternal leads," *Sensors*, vol. 17, no. 5, p. 1135, May 2017. [Online]. Available: http://www.mdpi.com/1424-8220/17/5/1135
[34] J. M. Bland and D. G. Altman, "Measuring agreement in method comparison studies," *Stat. Methods Med. Res.*, vol. 8, no. 2, pp. 135–160, Jun. 1999. [Online]. Available: http://journals.sagepub.com/doi/10.1177/096228029900800204
[35] D. Giavarina, "Understanding bland altman analysis," *Biochemia Medica*, vol. 25, no. 2, pp. 141–151, 2015. [Online]. Available: http://www.biochemia-medica.com/en/journal/25/2/10.11613/BM.2015.015
[36] J. Jezewski, A. Matonia, T. Kupka, D. Roj, and R. Czabanski, "Determination of fetal heart rate from abdominal signals: Evaluation of beat-to-beat accuracy in relation to the direct fetal electrocardiogram," *Biomedizinische Technik/Biomed. Eng.*, vol. 57, no. 5, pp. 383–394, Jan. 2012. [Online]. Available: https://www.degruyter.com/view/j/bmte.2012.57.issue-5/bmt-2011-0130/bmt%-2011-0130.xml
[37] A. L. Goldberger, L. A. N. Amaral, L. Glass, J. M. Hausdorff, P. C. Ivanov, R. G. Mark, J. E. Mietus, G. B. Moody, C.-K. Peng, and H. E. Stanley, "Physiobank, physiotoolkit, and physioNet: Components of a new research resource for complex physiologic signals," *Circulation*, vol. 101, no. 23, pp. e215–e220, Jun. 2000. [Online]. Available: https://www.ahajournals.org/doi/10.1161/01.CIR.101.23.e215
[38] T. Kazmi, F. Radfer, and S. Khan, "ST analysis of the fetal ECG, as an adjunct to fetal heart rate monitoring in labour: A review," *Oman Med. J.*, vol. 26, no. 6, pp. 459–460, Nov. 2011. [Online]. Available: http://www.omjournal.org/fultext_PDF.aspx?DetailsID=180&pdf=images/180% M_Deatials_Pdf_.pdf&type=pdf
[39] I. Amer-Wåhlin, C. Hellsten, H. Norén, P. H. Hagberg, A. Herbst, P. I. Kjellmer, H. Lilja, C. Lindoff, M. Månsson, L. Mårtensson, P. Olofsson, A.-K. Sundström, and K. Maršál, "Cardiotocography only versus cardiotocography plus ST analysis of fetal electrocardiogram for intrapartum fetal monitoring: A Swedish randomised controlled trial," *Lancet*, vol. 358, no. 9281, pp. 534–538, Aug. 2001. [Online]. Available: https://linkinghub.elsevier.com/retrieve/pii/S0140673601057038
[40] R. Kahankova, R. Martinek, R. Jaros, K. Behbehani, A. Matonia, M. Jezewski, and J. A. Behar, "A review of signal processing techniques for non-invasive fetal electrocardiography," *IEEE Rev. Biomed. Eng.*, vol. 13, pp. 51–73, 2019. [Online]. Available: https://ieeexplore.ieee.org/document/8820039/

KATERINA BARNOVA was born in Ostrava, Czech Republic, in 1993. She received the master's degree from the Department of Cybernetics and Biomedical Engineering, VSB-Technical University of Ostrava, in 2019, where she is currently pursuing the Ph.D. degree in technical cybernetics. Her research interests include advanced signal processing methods, especially for fECG extraction.

RADEK MARTINEK was born in Czech Republic, in 1984. He received the master's degree in information and communication technology from the VSB-Technical University of Ostrava, in 2009. Since 2012, he was working a Research Fellow with the VSB-Technical University of Ostrava. In 2014, he successfully defended his dissertation thesis titled The Use of Complex Adaptive Methods of Signal Processing for Refining the Diagnostic Quality of the Abdominal Fetal Electrocardiogram. He became an Associate Professor of technical cybernetics, in 2017, after defending the habilitation thesis titled Design and Optimization of Adaptive Systems for Applications of Technical Cybernetics and Biomedical Engineering Based on Virtual Instrumentation. He has been an Associate Professor with VSB-Technical University of Ostrava, since 2017. His current research interests include digital signal processing (linear and adaptive filtering, soft computing—artificial intelligence and adaptive fuzzy systems, non-adaptive methods, biological signal processing, digital processing of speech signals), wireless communications (software-defined radio), and power quality improvement. He has more than 200 journals and conference articles in his research areas.

RENE JAROS was born in 1992 in Ostrava, Czech Republic. He received the bachelor's degree from the Department of Cybernetics and Biomedical Engineering, VSB-Technical University of Ostrava, in 2015, the master's degree in biomedical engineering from the Department of Cybernetics and Biomedical Engineering, and the Ph.D. degree in technical cybernetics, in 2019. His research interests include fECG extraction by using hybrid methods.

RADANA KAHANKOVA was born in Opava, Czech Republic, in 1991. She received the bachelor's degree from the Department of Cybernetics and Biomedical Engineering, VSB-Technical University of Ostrava, in 2014, the master's degree in biomedical engineering from the Department of Cybernetics and Biomedical Engineering, and the Ph.D. degree in technical cybernetics, in 2019. Her current research interests includes on improving the quality of electronic fetal monitoring.